



This is a repository copy of *Damage-tolerant architected materials inspired by crystal microstructure*.

White Rose Research Online URL for this paper:
<http://eprints.whiterose.ac.uk/141436/>

Version: Supplemental Material

Article:

Pham, M.-S., Liu, C., Todd, I. orcid.org/0000-0003-0217-1658 et al. (1 more author) (2019) Damage-tolerant architected materials inspired by crystal microstructure. *Nature*, 565 (7739). pp. 305-311. ISSN 0028-0836

<https://doi.org/10.1038/s41586-018-0850-3>

© 2019 Springer Nature Limited. This is an author produced version of a paper subsequently published in *Nature*. Uploaded in accordance with the publisher's self-archiving policy.

Reuse

Items deposited in White Rose Research Online are protected by copyright, with all rights reserved unless indicated otherwise. They may be downloaded and/or printed for private study, or other acts as permitted by national copyright laws. The publisher or other rights holders may allow further reproduction and re-use of the full text version. This is indicated by the licence information on the White Rose Research Online record for the item.

Takedown

If you consider content in White Rose Research Online to be in breach of UK law, please notify us by emailing eprints@whiterose.ac.uk including the URL of the record and the reason for the withdrawal request.



eprints@whiterose.ac.uk
<https://eprints.whiterose.ac.uk/>

	Tensile modulus (MPa)	Tensile strength (MPa)	Elongation (%)
Ductile PLA *	3,310	110	160
Resin *	1,000 - 1,600	37 - 47	7 - 16
Natural FLEX 45 *	95	24	530
316L **	185,000 – 200,000	585	40 - 50

Table E1: Mechanical properties of printed polymers. * data provided by RS Limited and 3D Systems Limited. ** data obtained from 3 tensile tests of solid cylindrical samples (fabricated by powder-bed selective laser fusion) at room temperature and a strain rate of 10^{-3} 1/s).

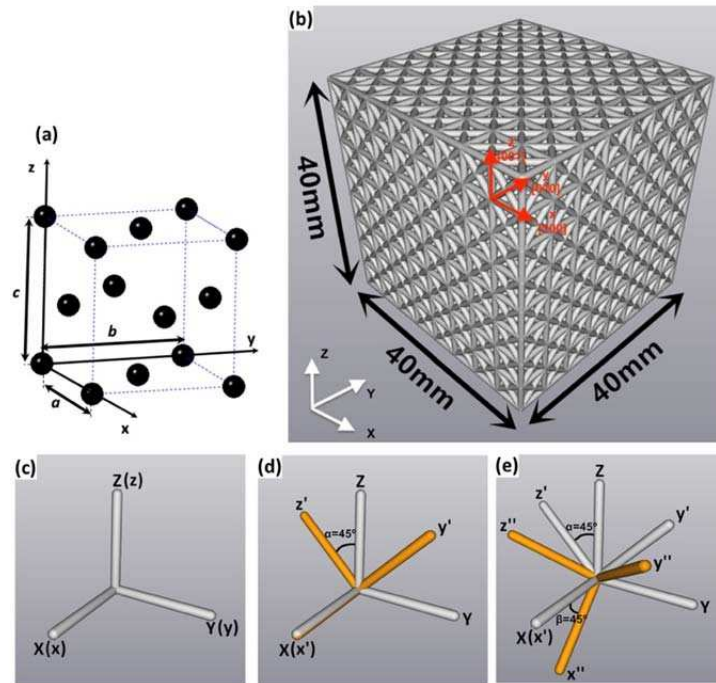


Figure E1: Mimicry of crystal lattice. (a) Unit cell of lattice, (b) A macro-lattice cube consisting of $8 \times 8 \times 8$ macro-unit cells. (c) – (e) The rotation sequence to form a twin meta-grain of lattice.

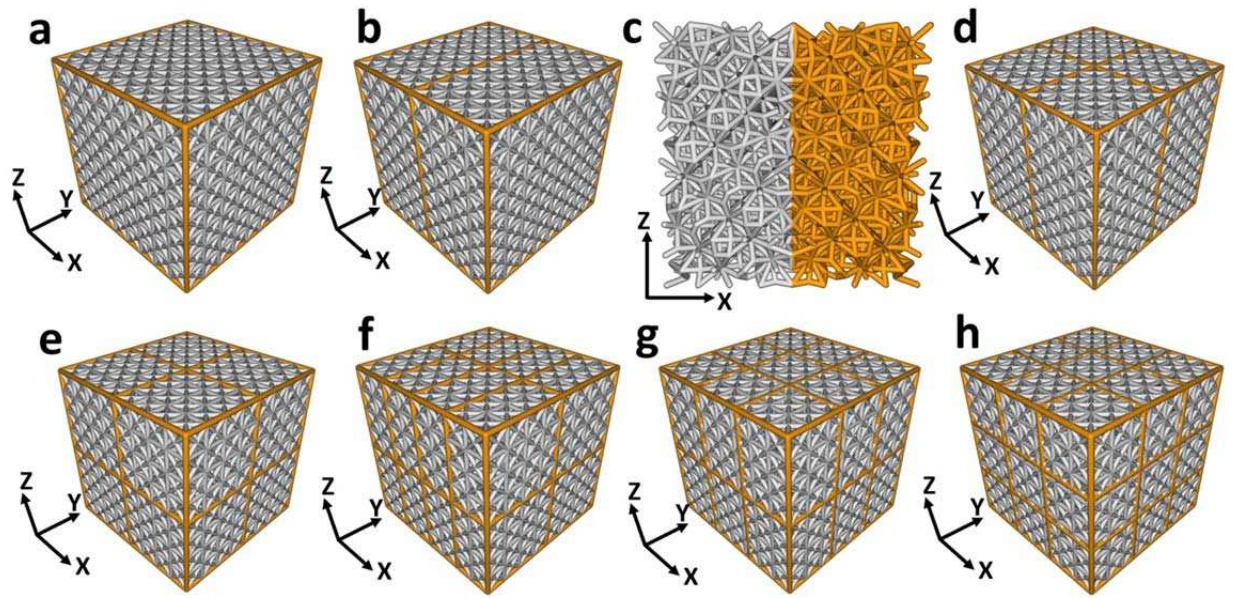


Figure E2: A different number of meta-grains within the same global volume (40mm x 40mm x 40mm). (a) 1 meta-grain, (b)-(c) 2 twinned meta-grains: (b) with outer frame and (c) without the outer frame, (d) 4 meta-grains, (e) 8 meta-grains, (f) 16 meta-grains, (g) 18 meta-grains and (e) 27 meta-grains. The locations of boundaries were highlighted.

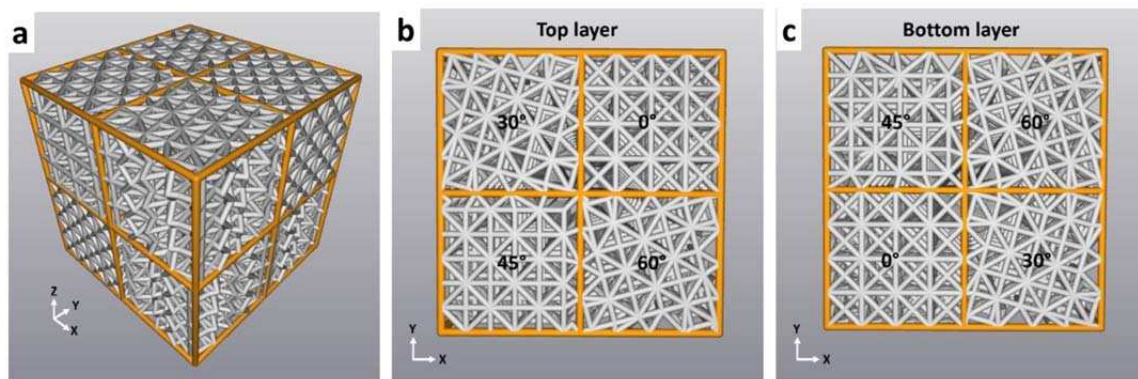


Figure E3: Mimicry of crystalline grains separated by incoherent high angle boundaries. (a) Model of 8 meta-grains. The orientations of lattices in the four meta-grains in (b) the top layer and (c) the bottom layer

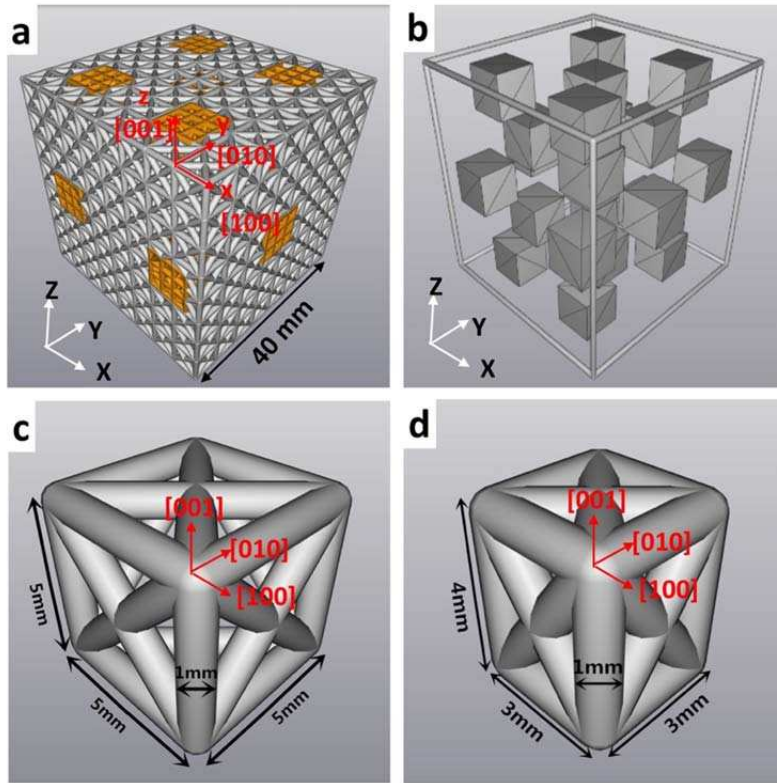


Figure E4: Mimicry of precipitates. (a) Meta-precipitate lattice. (b) Cubic morphology and locations of meta-precipitates inside the FCC meta-phase. (c) FCC unit cell of the matrix and (d) FCT unit cell of meta-precipitate.

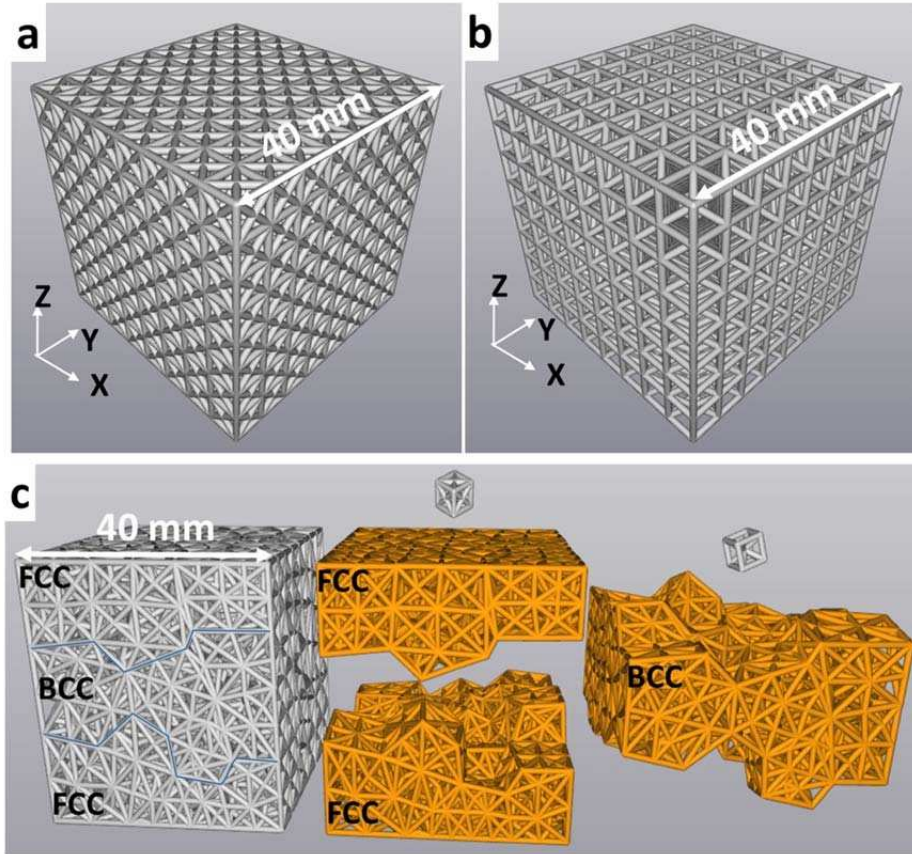


Figure E5: Mimicry of multi-phases. (a) Single meta-grain of FCC meta-phase, (b) Single meta-grain of BCC meta-phase, (c) A cube of meta-polygrains consisting of two meta-phases: FCC (top and bottom layers) and BCC (middle layer).

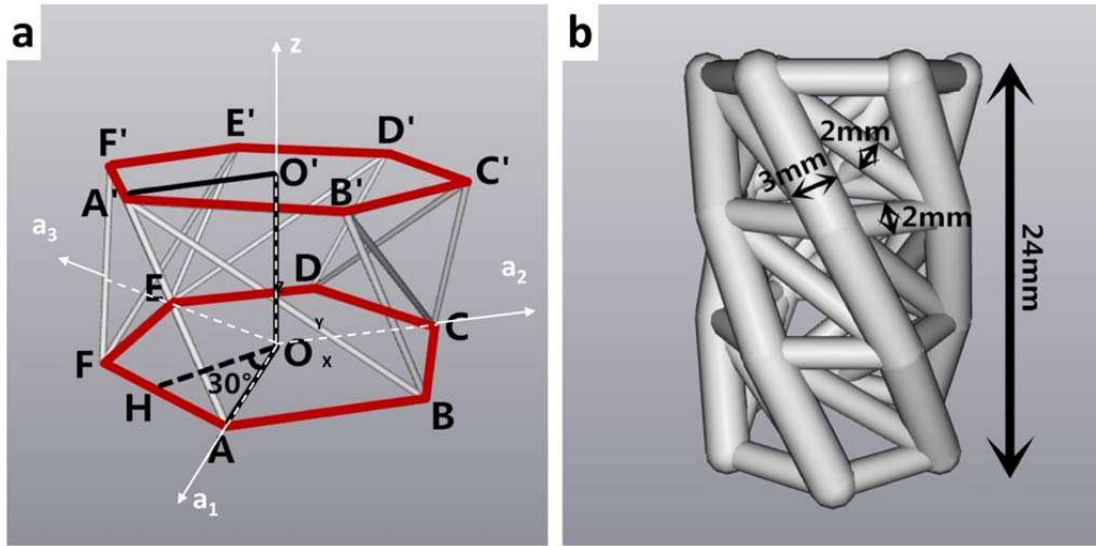


Figure E6: Kresling lattice. (a) unit cell, (b) HCP meta-phase

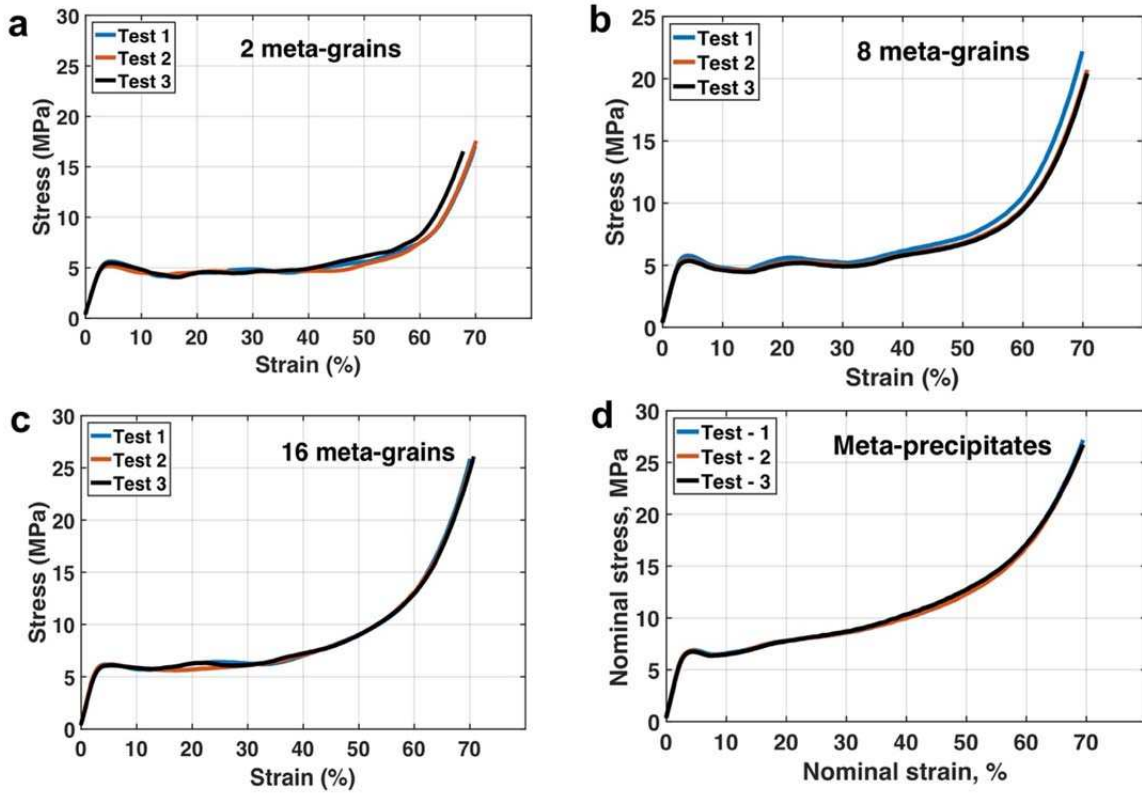


Figure E7: The repeatability of mechanical behaviour of architected materials. (a), (b) and (c) materials consist of 2, 8 and 16 meta-grains, respectively; and (d) materials contain 25 meta-precipitates.

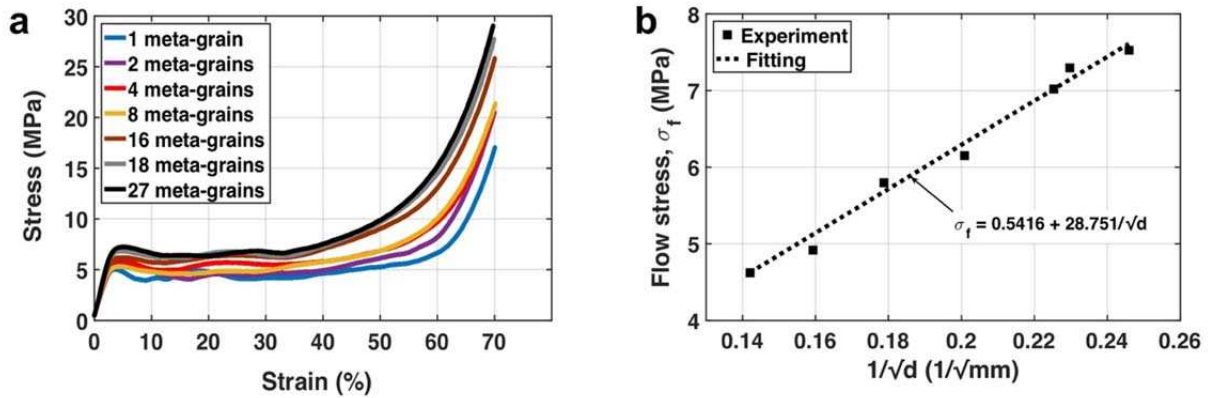


Figure E8: Effect of the size of meta-grains. (a) Stress-strain curves of architected materials consisting a different number of Voronoi domains of lattices. (b) Flow stress of architected materials containing meta-grains at a given nominal strain of 40% increases with reducing the size of meta-grains.

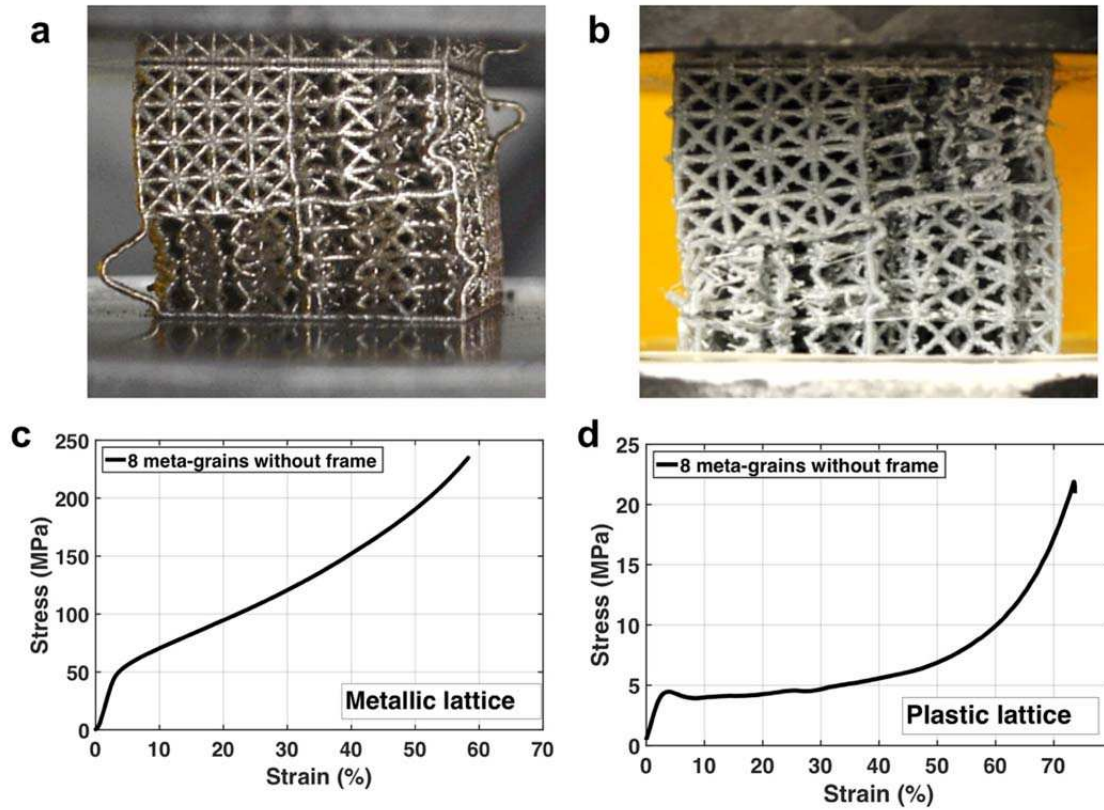


Figure E9: Deformation behaviours of an architected material containing 8 meta-grains separated by incoherent high angle boundaries. (a) and (b) the macro-lattice was fabricated by 316L stainless steel and elasto-plastic polymer, respectively. (c) and (d) stress-strain constitutive behaviour of the macro-lattices fabricated by the steel and polymer.

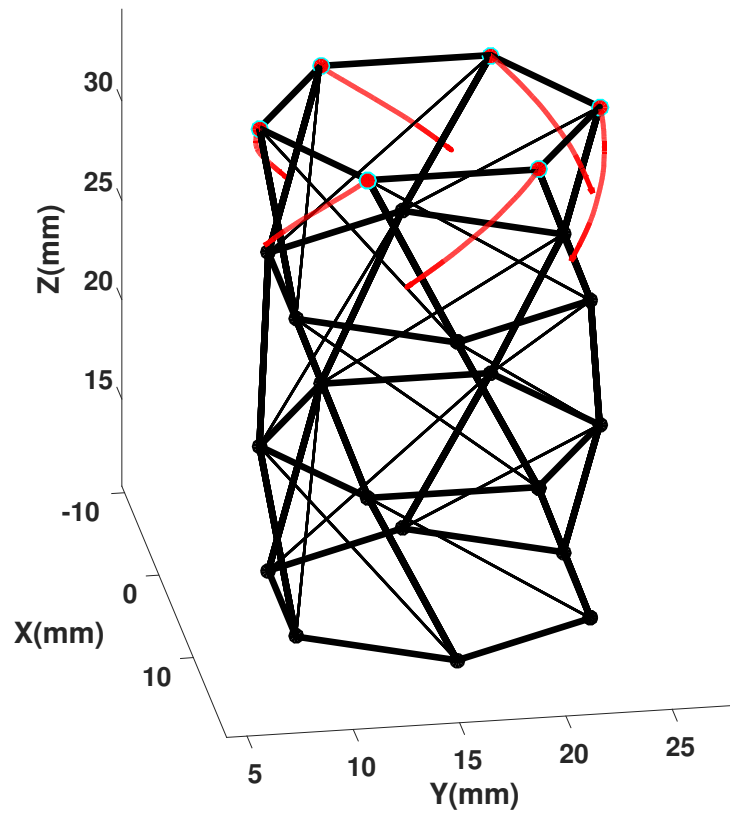


Figure E10: Helical movement enables the change in the stack sequence of nodes. Red lines represent helical movements of basal nodes. Note: only the movement trajectory of basal nodes on the top plane were shown by the red curves.